(12)

SC5361.6SAR

Copy No. 13

NONLINEAR WAVE PROPAGATION STUDY

SEMI-ANNUAL TECHNICAL REPORT NO. 2 FOR THE PERIOD December 1, 1983 through May 31, 1984

CONTRACT NO. F49620-83-C-0065
DARPA ORDER NO. 4400
PROGRAM CODE: 3A10

Prepared for

Air Force Office of Scientific Research
Building 410
Bolling AFB, DC 20332

Principal Investigator
B.R. Tittmann
(805) 498-4545

Sponsored by

Defense Advanced Research Projects Agency (DoD)
DARPA Order No. 4400
Monitored by NP Under Contract NO. F49620-83-C-0065

Rockwell International
Science Center

UNCLASSIFIED

SECURITY CLASSIFICATION OF THIS PAGE

REPORT DOCUMENTATION PAGE

1a. REPORT SECURITY CLASSIFICATION UNCLASSIFIED	1b. RESTRICTIVE MARKINGS
2a. SECURITY CLASSIFICATION AUTHORITY	3. DISTRIBUTION/AVAILABILITY OF REPORT Approved for public release; Distribution unlimited
2b. DECLASSIFICATION/DOWNGRADING SCHEDULE	
4. PERFORMING ORGANIZATION REPORT NUMBER(S) SC5361.6SAR	5. MONITORING ORGANIZATION REPORT NUMBER(S) AFOSR-TR- 84-0878
6a. NAME OF PERFORMING ORGANIZATION Rockwell International Science Center 6b. OFFICE SYMBOL (If applicable)	7a. NAME OF MONITORING ORGANIZATION AFOSR/NP
6c. ADDRESS (City, State and ZIP Code) 1049 Camino Dos Rios PO Box 1085 Thousand Oaks, CA 91360	7b. ADDRESS (City, State and ZIP Code) Building 410 Bolling AFB DC 20332-6448
8a. NAME OF FUNDING/SPONSORING ORGANIZATION AFOSR/NP 8b. OFFICE SYMBOL (If applicable) NP	9. PROCUREMENT INSTRUMENT IDENTIFICATION NUMBER F49620-83-C-0065
8c. ADDRESS (City, State and ZIP Code) Building 410 Bolling AFB DC 20332-6448	10. SOURCE OF FUNDING NOS. PROGRAM ELEMENT NO.: 62714E PROJECT NO.: 3A10 ~~4408~~ TASK NO.: 03 WORK UNIT NO.
11. TITLE (Include Security Classification) NONLINEAR WAVE PROPAGATION STUDY	
12. PERSONAL AUTHOR(S) B. R. Tittman	
13a. TYPE OF REPORT SEMI-ANNUAL TECH 13b. TIME COVERED FROM Dec 83 TO 31 May 84	14. DATE OF REPORT (Yr., Mo., Day) 31 May 84 15. PAGE COUNT 19
16. SUPPLEMENTARY NOTATION	
17. COSATI CODES FIELD / GROUP / SUB. GR.	18. SUBJECT TERMS (Continue on reverse if necessary and identify by block number)

19. ABSTRACT (Continue on reverse if necessary and identify by block number)

In this report the results of a study of the response of Westerly granite to sinusoidal loading, are presented. The amplitude of transition from linearity to non-linearity can be defined. Results are compared to previous studies.

20. DISTRIBUTION/AVAILABILITY OF ABSTRACT UNCLASSIFIED/UNLIMITED ☒ SAME AS RPT. ☐ DTIC USERS ☐	21. ABSTRACT SECURITY CLASSIFICATION UNCLASSIFIED
22a. NAME OF RESPONSIBLE INDIVIDUAL Dr. Henry R. Radoski	22b. TELEPHONE NUMBER (Include Area Code) 202/767-4906 22c. OFFICE SYMBOL NP

DD FORM 1473, 83 APR EDITION OF 1 JAN 73 IS OBSOLETE.

UNCLASSIFIED

SECURITY CLASSIFICATION OF THIS PAGE

TABLE OF CONTENTS

LIST OF FIGURES

1.0 INTRODUCTION

At the present time there still exists an element of uncertainty regarding the definition of an effective radius, which can be used to separate the nonlinear near-field regime adjacent to an explosion from the linear far-field seismic regime. Using data sets from the COWBOY experiments and the SALMON test Trulio (1978, 1981) studied the decay of peak particle velocity as a function of scaled distance in dome salt. He observed that decay rates are significantly faster than can be explained assuming perfectly elastic behavior, and concluded that material behavior was not perfectly elastic, and probably nonlinear, even at strains as low as those encountered at the most distant instruments. Larson (1982) examined near-field particle motions in pressed salt in the laboratory using small-scale chemical explosions. He demonstrated near-linear superposition of wave forms even at strains in excess of 10^{-4}. Yet, the Q values calculated by Larson (12.5 near 10^{-3} strain and 24.9 near 6 10^{-4} strain) depended on amplitude, indicating nonlinear behavior. Furthermore, these values are low compared with those measured by Tittmann (1983a) using the same material except at much lower amplitudes. The work of Tittmann (1983a, 1983b) demonstrates that nonlinear effects, as reflected in an amplitude-dependent Q, can persist to very low levels of strain, even below 10^{-6} in some cases. More recently, Minster (1982) and Minster and Day (1984) re-examined the COWBOY data and concluded that the observed decay rates can only be explained using an amplitude dependent Q. However, Burdick et al (1984a) have argued that it is possible to model a seismic source function for the Amchitka tests assuming linear behavior in the near field just outside the spall zone (approx. 700-1200 m/kt$^{1/3}$). Furthermore, Burdick et al (1984b) argued that the same model can be used to predict the first vertical pulse arrival and rise times even within the spall zone. They used the concept of a compressional elastic radius, which may in fact be considerably less than a tensional elastic radius, which must extend at least as far as the outer limits of the spall zone.

In this report we present the results of a recent study of the response of Westerly granite to sinusoidal loading. The amplitude of transition from linearity to nonlinearity can be defined, and results are compared to previous studies.

2.0 EXPERIMENTAL STUDIES

The techniques used to obtain the data presented in this report are the same as those described in an earlier report (Tittmann, 1983a). Briefly, a cylindrical specimen of Westerly granite, 13 cm in length and 0.71 cm in radius, was clamped into an apparatus which enabled it to be vibrated in both flexural and torsional modes. In this particular study the resonant frequency was between 500 and 550 Hz for all measurements. The Q of the bar could be calculated from the ratio of the resonant frequency to the bandwidth of the resonance curve. The voltage of the electromagnetic transducer, used to drive the resonance, could be adjusted so as to vary the amplitude of vibration (vibration amplitudes for torsional and flexural vibrations are defined in Fig. 1). Thus, attenuation (Q^{-1}) and RMS driving voltage can be measured as a function of vibration amplitude in the sample. Provided that the sample behaves linearly, the attenuation should be independent of vibration amplitude, and the RMS driving voltage should be proportional to vibration amplitude (c.f. Tittmann, 1983a). Measurements were made in both wet and dry Westerly granite at effective pressures from 0 to 34 MPa.

The results of this study are shown in Figs. 2-21. The results are qualitatively consistent with the results of previous studies (Tittmann, 1983a) in that linear behavior is observed at all low amplitudes, with a transition for nonlinear behavior at high strain. The transition amplitude is near 10^{-6} in all cases, including both torsion and flexure, increasing very slightly with increasing effective pressure.

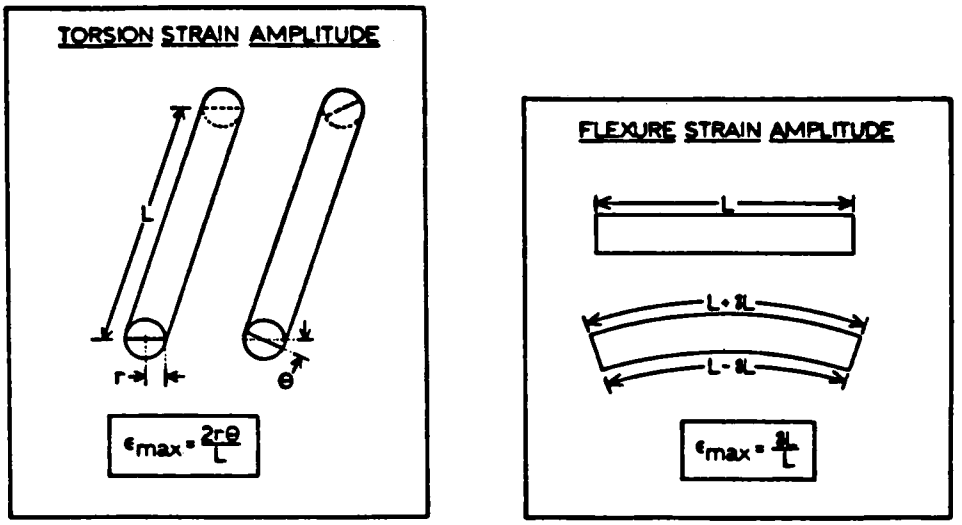

Fig. 1 Definition of strain amplitude in fluxure and torsion.

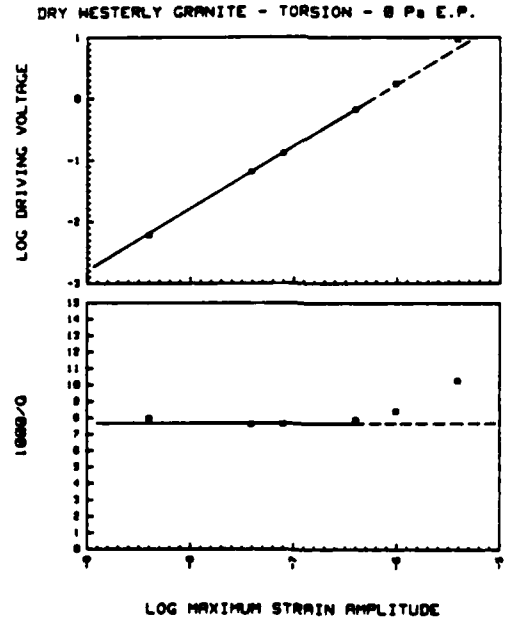

Fig. 2 Attenuation and log RMS driving transducer voltage plotted as a function of strain amplitude for torsional vibrations in dry Westerly granite at 0 MPa effective pressure.

SC5361.6SAR

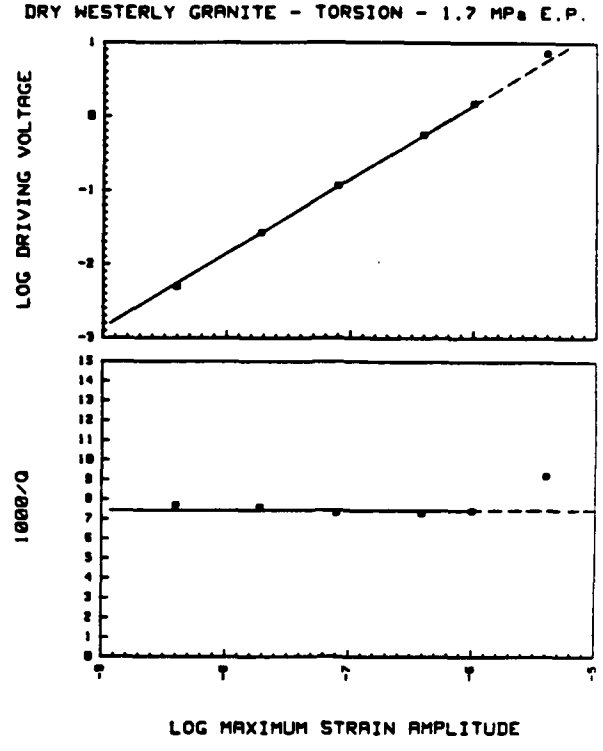

Fig. 3 Attenuation and log RMS driving transducer voltage plotted as a function of strain amplitude for torsional vibrations in dry Westerly granite at 1.7 MPa effective pressure.

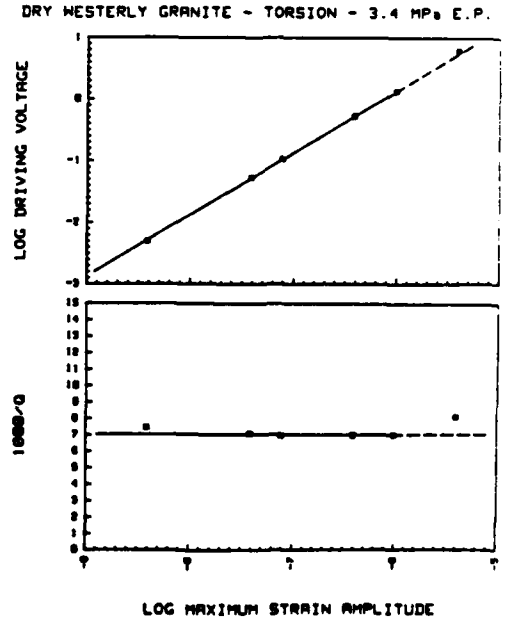

Fig. 4 Attenuation and log RMS driving transducer voltage plotted as a function of strain amplitude for torsional vibrations in dry Westerly granite at 3.4 MPa effective pressure.

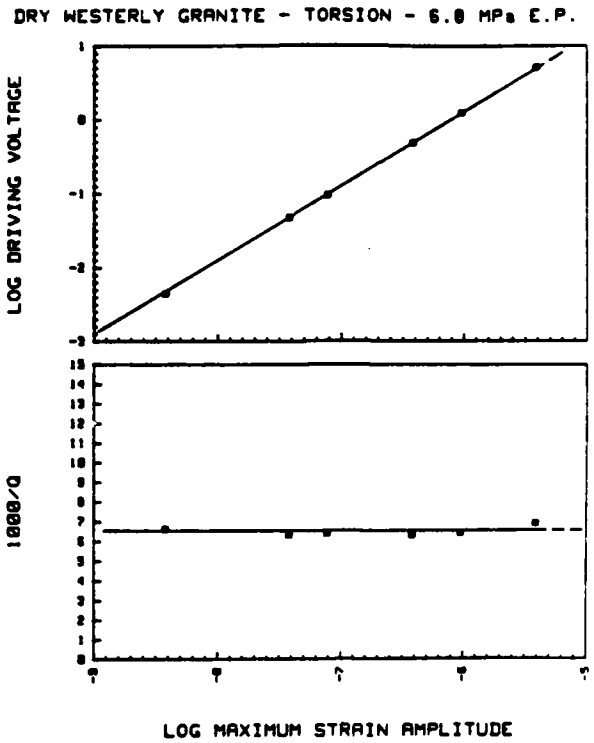

Fig. 5 Attenuation and log RMS driving transducer voltage plotted as a function of strain amplitude for torsional vibrations in dry Westerly granite at 6.8 MPa effective pressure.

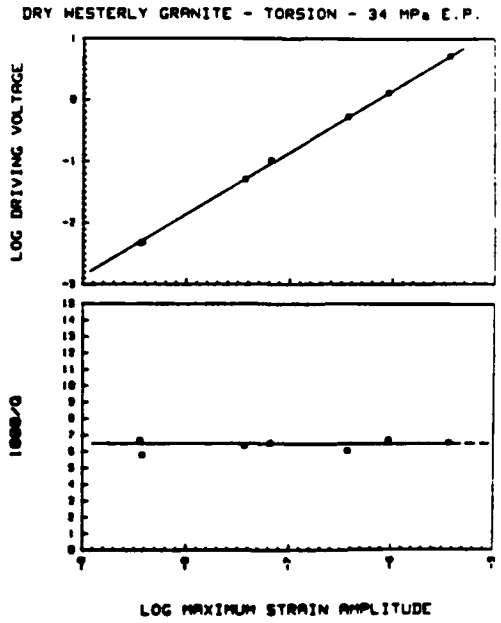

Fig. 6 Attenuation and log RMS driving transducer voltage plotted as a function of strain amplitude for torsional vibrations in dry Westerly granite at 34 MPa effective pressure.

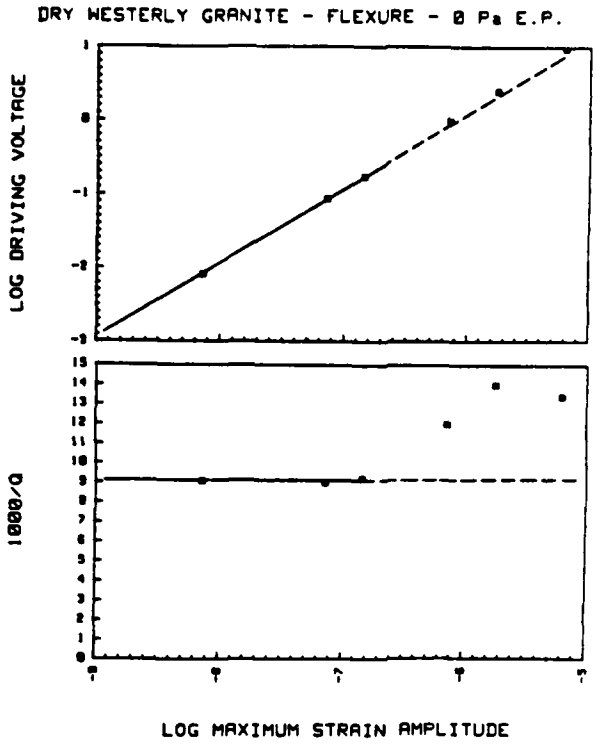

Fig. 7 Attenuation and log RMS driving transducer voltage plotted as a function of strain amplitude for flexural vibrations in dry Westerly granite at 0 MPa effective pressure.

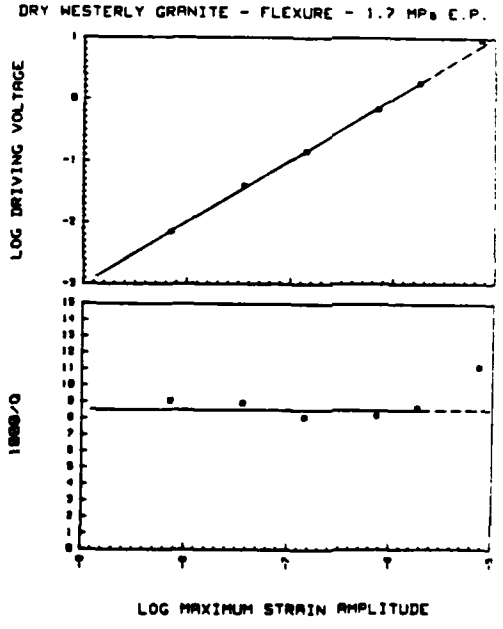

Fig. 8 Attenuation and log RMS driving transducer voltage plotted as a function of strain amplitude for flexural vibrations in dry Westerly granite at 1.7 MPa effective pressure.

SC5361.6SAR

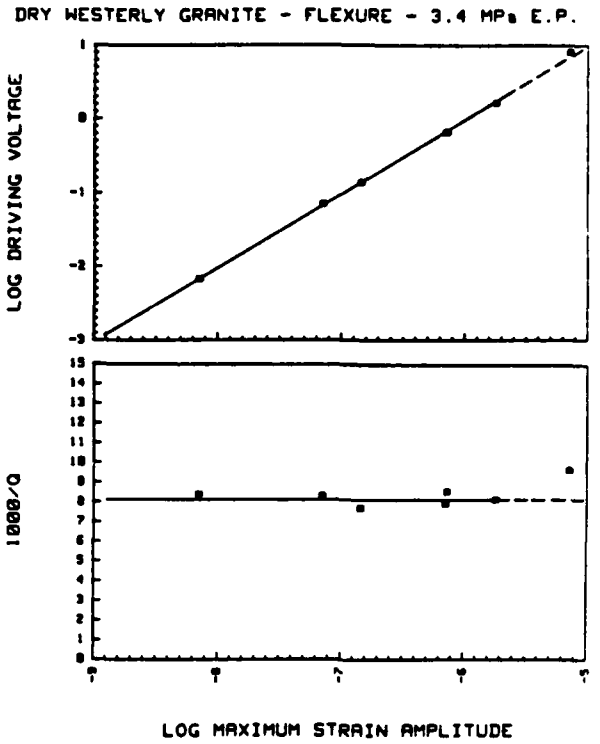

Fig. 9 Attenuation and log RMS driving transducer voltage plotted as a function of strain amplitude for flexural vibrations in dry Westerly granite at 3.4 MPa effective pressure.

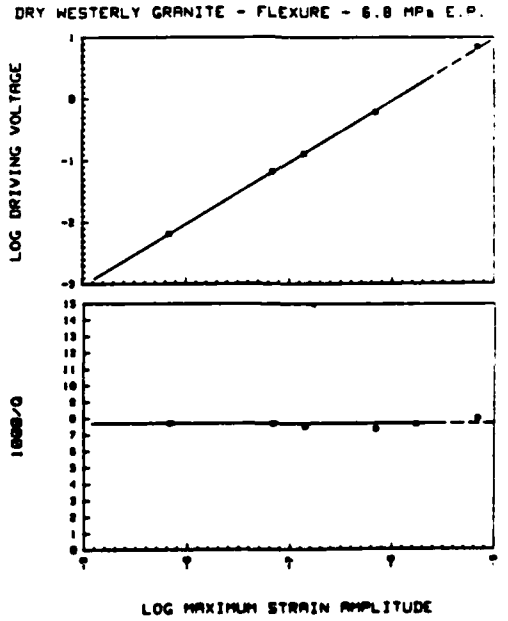

Fig. 10 Attenuation and log RMS driving transducer voltage plotted as a function of strain amplitude for flexural vibrations in dry Westerly granite at 6.8 MPa effective pressure.

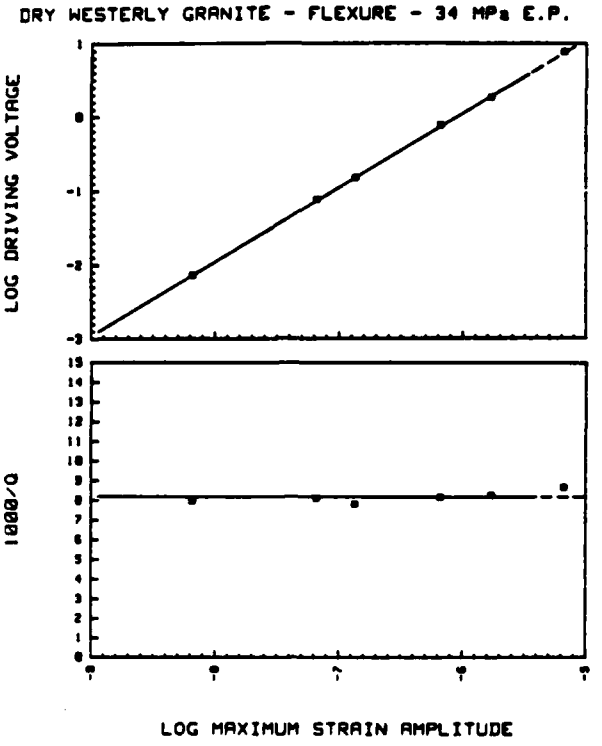

Fig. 11 Attenuation and log RMS driving transducer voltage plotted as a function of strain amplitude for flexural vibrations in dry Westerly granite at 34 MPa effective pressure.

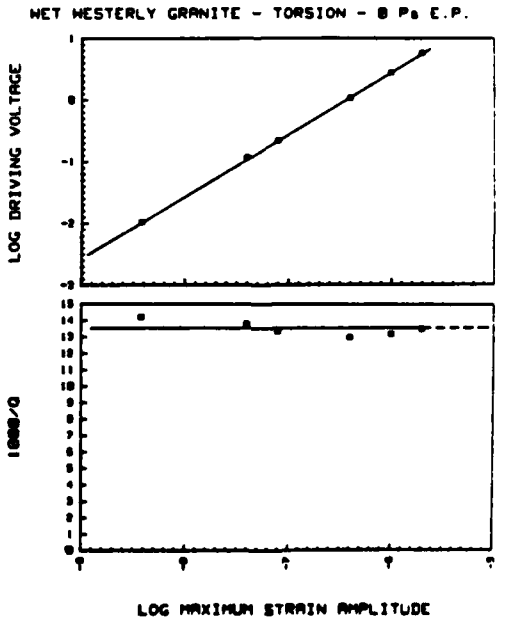

Fig. 12 Attenuation and log RMS driving transducer voltage plotted as a function of strain amplitude for torsional vibrations in wet Westerly granite at 0 MPa effective pressure.

SC5361.6SAR

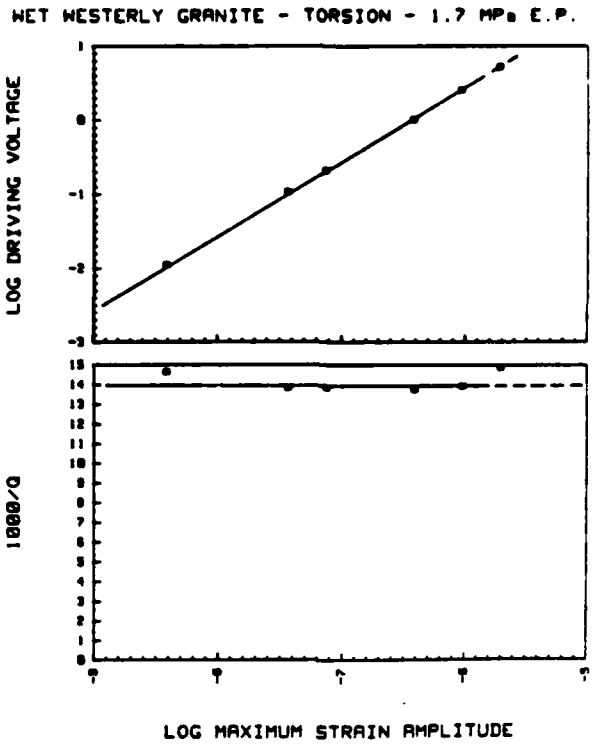

Fig. 13 Attenuation and log RMS driving transducer voltage plotted as a function of strain amplitude for torsional vibrations in wet Westerly granite at 1.7 MPa effective pressure.

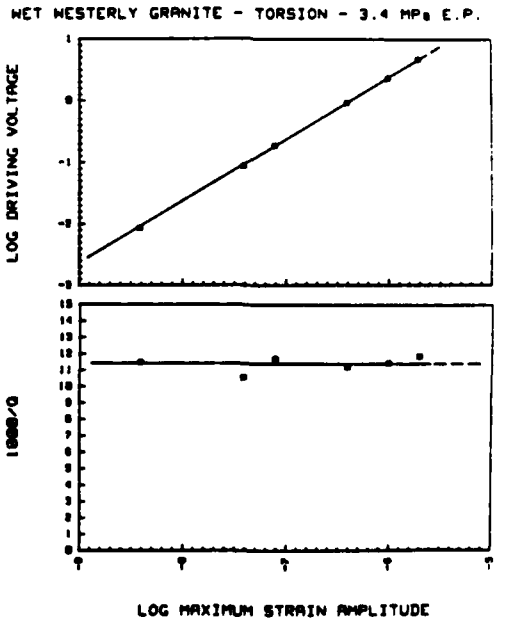

Fig. 14 Attenuation and log RMS driving transducer voltage plotted as a function of strain amplitude for torsional vibrations in wet Westerly granite at 3.4 MPa effective pressure.

SC5361.6SAR

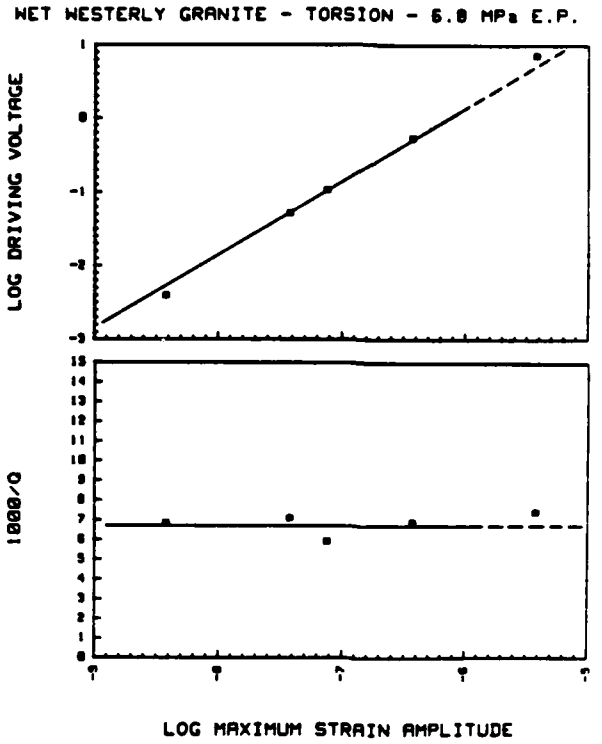

Fig. 15 Attenuation and log RMS driving transducer voltage plotted as a function of strain amplitude for torsional vibrations in wet Westerly granite at 6.8 MPa effective pressure.

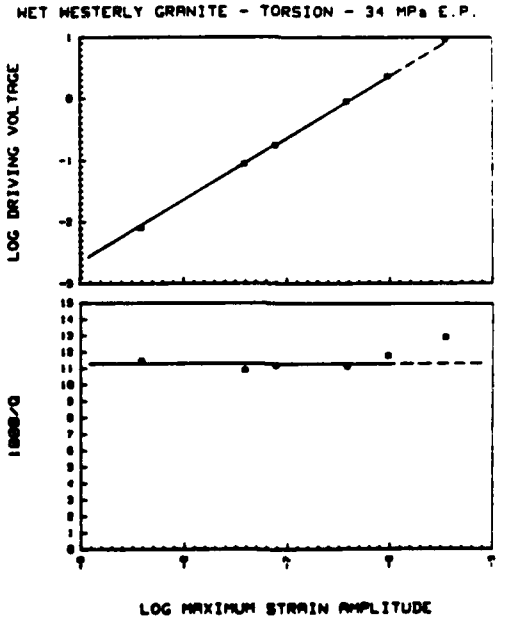

Fig. 16 Attenuation and log RMS driving transducer voltage plotted as a function of strain amplitude for torsional vibrations in wet Westerly granite at 34 MPa effective pressure.

SC5361.6SAR

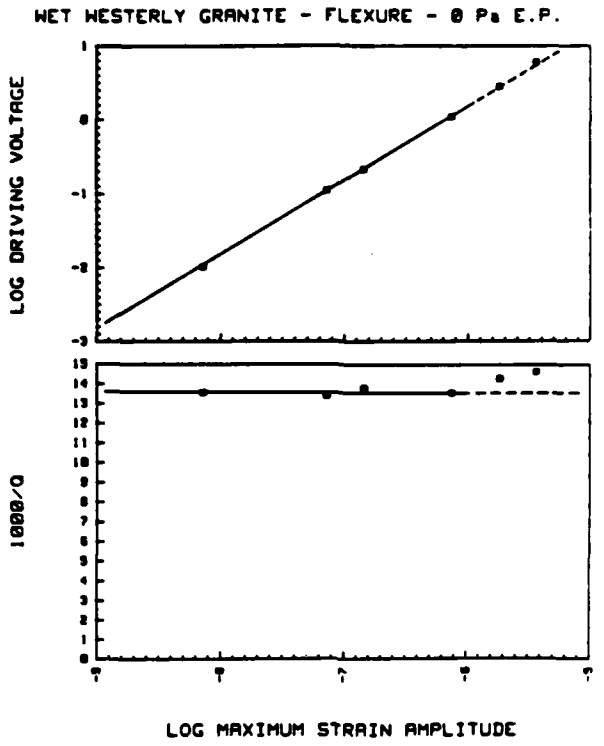

Fig. 17 Attenuation and log RMS driving transducer voltage plotted as a function of strain amplitude for flexural vibrations in wet Westerly granite at 0 MPa effective pressure.

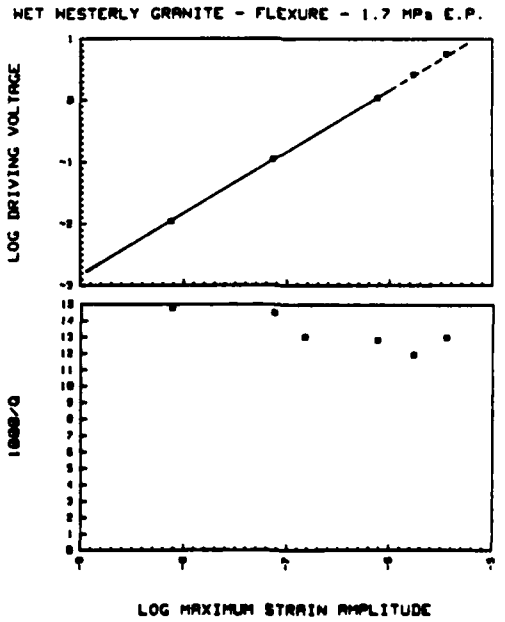

Fig. 18 Attenuation and log RMS driving transducer voltage plotted as a function of strain amplitude for flexural vibrations in wet Westerly granite at 1.7 MPa effective pressure.

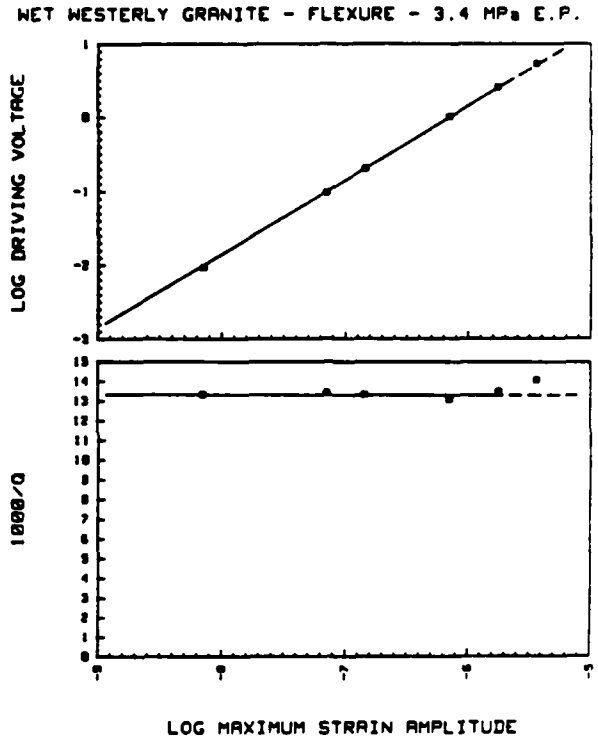

Fig. 19 Attenuation and log RMS driving transducer voltage plotted as a function of strain amplitude for flexural vibrations in wet Westerly granite at 3.4 MPa effective pressure.

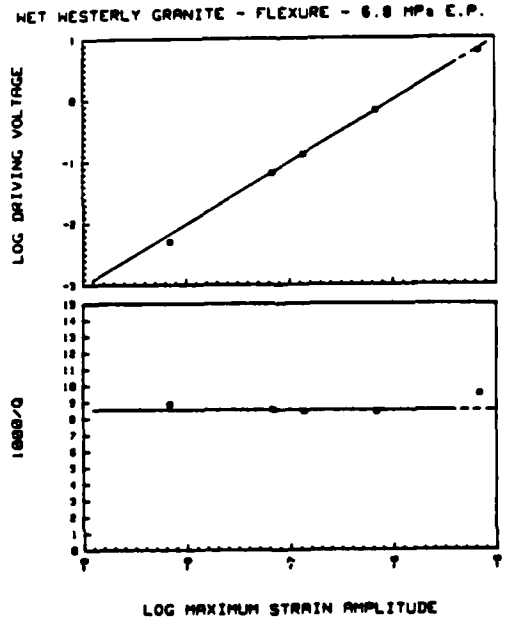

Fig. 20 Attenuation and log RMS driving transducer voltage plotted as a function of strain amplitude for flexural vibrations in wet Westerly granite at 6.8 MPa effective pressure.

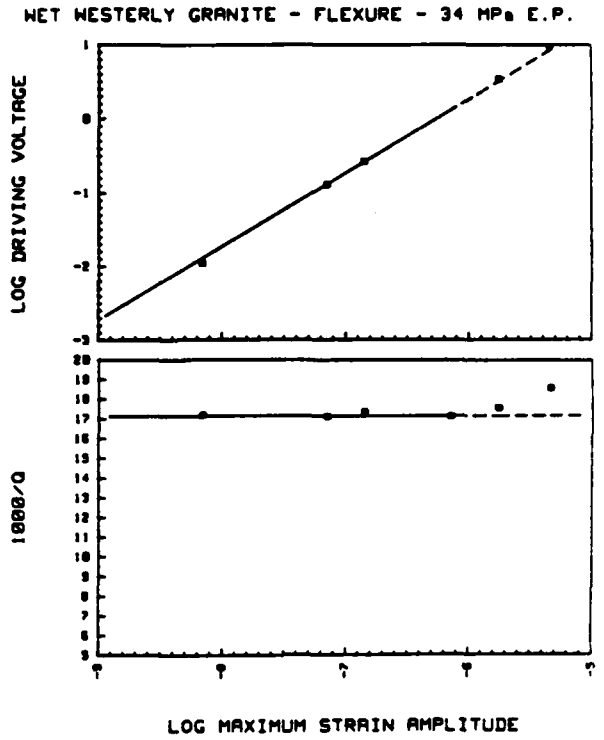

Fig. 21 Attenuation and log RMS driving transducer voltage plotted as a function of strain amplitude for flexural vibrations in wet Westerly granite at 34 MPa effective pressure.

3.0 DISCUSSION

In this phase of the study, as in those presented earlier, the test specimen was subjected to a long train of sinusoidal vibrations. For flexural vibrations the test material spent half of its cycle primarily in tension and half of its cycle primarily in compression. Therefore, using this type of measuring technique with harmonic vibrations it is not possible to establish whether the nonlinearity observed in the flexural mode data is due to relaxation in compression, relaxation in tension, or both. Recognizing the fact that rocks are significantly stronger in compression than in tension it is reasonable to expect that the nonlinearity is primarily a tensional phenomenon, but this remains to be established experimentally. More data on the constitutive properties of rocks at modest amplitudes (10^{-4} to 10^{-6}) are required. An ideal study would include measurements in both uniaxial compression and uniaxial tension. Other issues regarding the applicability of the

resonating bar technique for simulating non-linear pulse loading are discussed in the previous report (Tittman, 1983b), and will not be repeated here.

It is quite reasonable to assume that the amplitude of transition from linear to nonlinear behavior detected with the resonating bar apparatus represent a lower limit on the corresponding transition amplitude for a seismic pulse propagating in the near-field of an explosion. The accumulated damage caused by subjecting the specimen to repeated cycles of high amplitude vibration (Tittmann, 1983b) would have the effect of making the transition amplitude appear relatively low in laboratory experiments compared with the field. Furthermore, the material near the explosion is subjected to lower levels of tensional stress than compressional stress, and tensional nonlinearity may occur at lower stress levels than compressional nonlinearity.

Measurements of the constitutive properties of materials in both tension and compression are critical and will be included in future studies.

4.0 SUMMARY AND CONCLUSIONS

Nonlinear effects have been observed in a cylindrical test specimen of Westerly granite which was subjected to both flexural and torsional modes of resonant vibration. Nonlinear effects in shear are observed when the shearing strain exceeds approximately 10^{-6}, increasing slightly with increasing effective pressure. Nonlinear effects in flexure are also observed when the extension/compression strain exceeds 10^{-6}, also increasing very slightly with increasing effective pressure. These transition amplitudes probably represent a lower limit on the amplitude of transition from linear to nonlinear behavior for the primary elastic pulse propagating in the near-field of an explosion. Using these measurements it is not possible to determine whether the nonlinear effects observed in flexure are primarily an extensional or compressional feature. This is a critical issue and in future studies we will attempt to examine the constitutive properties of rocks in both tension and compression under moderate to low amplitude conditions.

5.0 REFERENCES

Burdick, L.J., T. Wallace and T. Lay (1984a), Modeling Near-Field and Teleseismic Observations from the Amchitka Test Site, Jour. Geophys. Res., 89, 4373-4388.

Burdick, L.J., T Lay, D.V. Helmberger, and D.G. Harkrider (1984b), Implications of Records from the Spall one of the Amchitka Tests to Nonlinear Losses in the Source Region and to Elastic Radiation by Spall. Annual technical report for the period November 15, 1982 to November 15, 1983. Prepared for the Advanced Research Projects Agency.

Larson, D.B. (1982), Inelastic Wave Propagation in Sodium Chloride, Bull. of the Seismological Soc. Amer., 72, 1207-1230.

Minster, J.B. (1982), Effects of Near-Field Nonlinear Attenuation on Outgoing Seismic Wavefields (abstract), Terra Cognita, 2, 153.

Minster, J.B. and S.M. Day (1984) High Strain, Nonlinear Attenuation in Salt and Its Effect on Outgoing Wavefields, in preparation.

Tittmann, B.R. (1983a), Studies of Absorption in Salt, Final Report for the Period Dec. 1, 1981 through Nov. 30, 1982. Prepared for Air Force Office of Scientific Research under contract Number F49620-82-C-0015.

Tittmann, B.R. (1983b), Non-Linear Wave Propagation Study, Semi-Annual Report for the Period June 1, 1983 through Nov. 30, 1983. Prepared for AFOSR under contract number F49620-83-C-0065.

Trulio J.G. (1978), Simple Scaling and Nuclear Monitoring, Final Report of DARPA supported research program, April 1978.

Trulio, J.G. (1981), State-of-the-Art Assessment: Seismic Yield Determination, in A Technical Assessment of Seismic Yield Estimation, DARPA Report Appendix, January, 1981.